Journal of Coastal Research	SI	113	624-628	Charlotte, North Carolina	2024

Hydrodynamic Analysis of an Oscillating Water Column Wave Energy Converter

Nagi Abdussamie[†]*, Thiban Subramaniam[‡], Aiyad Gannan[†], and Wesam Rohouma[†]

[†]College of Engineering and Technology
University of Doha for Science and Technology
Doha, Qatar

[‡]Centre for Maritime Engineering and Hydrodynamics
Australian Maritime College, University of Tasmania
Launceston, Tasmania, Australia

www.cerf-jcr.org

www.JCRonline.org

ABSTRACT

Abdussamie, N., Subramaniam, T., Gannan, A., and Rohouma W., 2024. Hydrodynamic analysis of an oscillating water column wave energy converter. *In:* Phillips, M.R.; Al-Naemi, S., and Duarte, C.M. (eds.), *Coastlines under Global Change: Proceedings from the International Coastal Symposium (ICS) 2024 (Doha, Qatar)*. *Journal of Coastal Research*, Special Issue No. 113, pp. 624-628. Charlotte (North Carolina), ISSN 0749-0208.

Wave energy offers a promising renewable energy source with added benefits for coastal protection. This study investigates the hydrodynamic performance of a fixed Oscillating Water Column (OWC) Wave Energy Converter (WEC) under different wave conditions, focusing on wave period, wave height, and device draft. The obtained results show that peak hydrodynamic efficiency occurs at the natural frequency of the water column and decreases with increased draft due to reduced water mass in the OWC chamber. This highlights the need for thorough evaluation of site-specific wave conditions for optimal power extraction. These findings are crucial for the geometry optimization and site selection of fixed OWC devices, contributing to the advancement of wave energy conversion technology and sustainable energy solutions.

ADDITIONAL INDEX WORDS: *Renewable energy, wave energy, model testing, oscillating water column.*

INTRODUCTION

For decades, the world has relied heavily on fossil fuels to meet the vast energy requirements of an expanding population. However, recent global events on sustainability have highlighted the risks associated with the use of fossil fuels for energy generation, including increased costs, depleting reserves, significant environmental impacts, and the acceleration of climate change due to greenhouse gas emissions. In response, there has been a growing focus on developing the renewable energy industry. Marine and offshore renewable energies hold significant potential for sustainable energy generation and coastal protection. Harnessing the power of waves, tides, and offshore wind can provide a substantial portion of the world's energy needs while reducing dependence on fossil fuels.

Wave energy converters (WECs) have been a topic of interest in the renewable energy sector since the 1980s, with oscillating water columns (OWCs) being a consistent design. OWC development began in Japan as early as the 1940s, with Kaimei, the first large-scale WEC, being deployed at sea in 1978, designed by Yoshio Masuda (Falcão & Henriques, 2016). As the global energy sector moves away from non-renewables, there is a trend towards the commercial implementation of various renewable devices to mitigate climate change. However, only a handful of OWC devices have been constructed and installed for commercial use worldwide (Singh et al., 2020), primarily due to a limited understanding of their hydrodynamics, necessitating further investigations.

The objective of the present study is to investigate the hydrodynamic efficiency of a fixed OWC device under varying drafts and different wave conditions, including regular and irregular waves. By examining the influence of wave period, wave height, and device draft on the OWC's performance, this research aims to enhance the understanding and optimization of OWC devices, contributing to the advancement of wave energy conversion technology.

METHODS

Theory

In the context of hydrodynamics, when a small amplitude surface wave interacts with an OWC WEC, the overall power extraction efficiency (ξ) can be estimated as:

$$\xi = \frac{P_{out}}{P_{in}} \tag{1}$$

The mean absorbed pneumatic power P_{out} per unit width (W/m) is estimated by integrating the product of air pressure measured in the OWC chamber $P(t)$ and the normal vertical velocity of free surface inside the OWC chamber $V(t)$ over the duration of t_s

$$P_{out} = \frac{L}{t_s}\int_0^{t_s} P(t)\cdot V(t)dt \tag{2}$$

where L is the OWC chamber length.

DOI: 10.2112/JCR-SI113-123.1 received 23 June 2024; accepted in revision 30 July 2024.
*Corresponding author: nagi.abdussamie@udst.edu.qa

As the air velocity $V(t)$ is estimated from the inner free surface elevation of OWC, the effect of air compressibility is ignored. Based on wave theory, the average energy flux per unit width in the incident wave is given by (DNV, 2010):

$$P_{\text{in}} = \frac{1}{8}\rho g H^2 C_g \tag{3}$$

where ρ is the water density, g is the gravitational acceleration, H is the incident wave height and C_g is the group velocity of the incident wave.

For a moonpool with constant cross-sectional area A_{owc} the natural period in heave is given by (DNV, 2010):

$$T_{owc} = 2\pi\left(\frac{h_{owc} + \kappa\sqrt{A_{owc}}}{g}\right)^{\frac{1}{2}} \tag{4}$$

where h_{owc} is the height of the water column. The factor κ depends on the cross-sectional shape of the water column (δ = breadth/length). The factor κ for a general rectangular moonpool (for $0 < \delta < 1$) is given by (Molin, 2001) :

$$\kappa = \frac{\sqrt{\delta}}{\pi}\left[\sinh^{-1}(\delta^{-1}) + (\delta^{-1})\sinh^{-1}\delta + \frac{1}{3}(\delta + \delta^{-2}) - \frac{1}{3}(1 + \delta^{-2})\sqrt{1 + \delta^2}\right] \tag{5}$$

The motion of the water in the OWC chamber has a resonance at a wave frequency corresponding to the eigenfrequency of a vertically oscillating water column.

Physical Model Testing

The data and results generated in this investigation were derived experimentally by tank testing of a scaled model OWC device. Tank testing provides a faster and more repeatable method compared to at sea testing and can emulate scaled extreme events to better understand and mitigate their effects. This investigation tested a 1:36 scaled model OWC at constant water depth and a range of wave periods and wave heights. Several runs per wave sea state were undertaken to allow the generation of a reliable average hydrodynamic efficiency.

OWC Model and Test Matrix

The OWC device used in this experimental study is illustrated below in Figure 1. A model scale of 1:36 was ultimately decided based on the available water depth at the testing facility (800 mm) resulting in a full-scale water depth of 28.8 m.

The OWC model was constructed from 7 mm thick wood ply, and featured an open bottom flume chamber, bounded by a full-length back wall and two fully enclosed side chambers. The total draft from the device base is 408 mm. The interior dimensions of the chamber at the designed h_{owc} of 100 mm are measured as 265 mm x 252 mm x 222 mm, for the width, length, and height respectively. As illustrated in Figure 2, the front wall draft (h_{owc}) of the OWC was varied during the experimental testing program from 75 mm to 175 with a 25 mm increment to study its effect on the device performance.

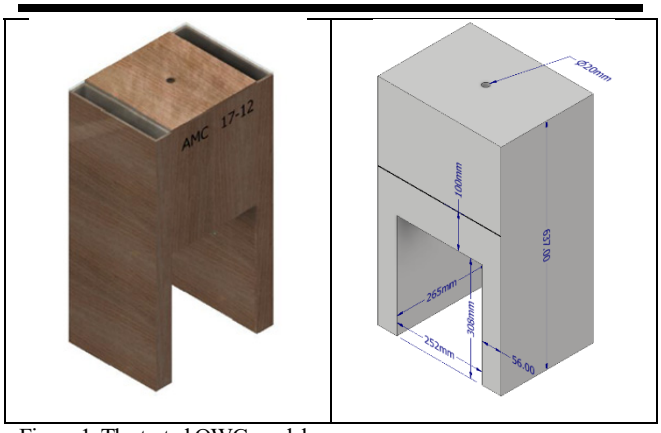

Figure 1. The tested OWC model.

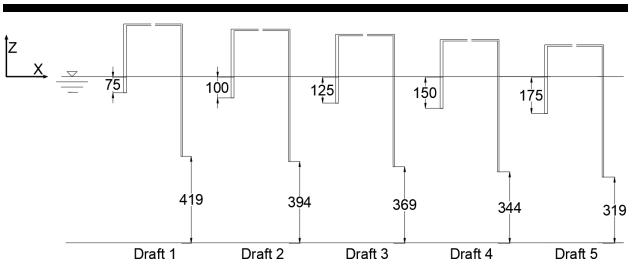

Figure 2. A profile view showing model's drafts (dimensions are in mm) [not to scale].

The wave test conditions were based on real sites in the east coast of Australia such as Crowdy Head, Eden, Byron Bay and Sydney as shown in Figure 3. The full-scale significant wave height, H_s varies from 1.38 m to 1.96 m and the associated peak period, T_p varies from 7.31 s to 8.45 s. The JONSWAP spectrum with a peak shape parameter γ=1.0, which is identical to the Pierson–Moskowitz (PM) spectrum, was used to synthesize short-time wave trains. The PM spectrum is commonly adopted formulation of the fully developed wind-generated wave elevation spectrum for different offshore locations. Scaled wave heights (H) ranged from 38 mm – 54 mm with peak periods ranged from 1.22 s – 1.41 s were tested. The test conditions for the selected sea states are given in Table 1.

Testing Facility

The model testing campaign was conducted at the Australian Maritime College Model Test Basin (AMC MTB). The basin is 35 m long, 12 m wide and capable of water depth of up to 1 m. The basin utilizes a wave maker consisting of 16 computer-controlled paddles (piston-type) to produce both regular and irregular waves. Figure 4 illustrated the model setup arrangement in which five wave probes (denoted as WP) and an air pressure sensor (denoted as APS) were used in the experiments. Data was acquired at a sampling frequency of 200 Hz for approximately 40 s – 60 s for each run.

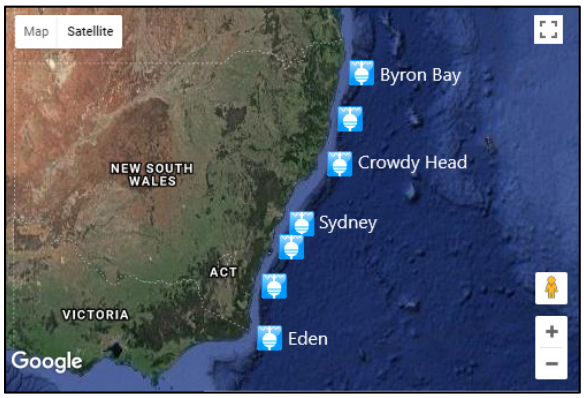

Figure 3. Satellite view of test sites.

Table 1. *Wave conditions.*

Sea state	Full-scale		Model-scale (1:36)	
	H_s (m)	T_p (s)	H_s (m)	T_p (s)
1	1.38	8.01	0.038	1.335
2	1.79	7.31	0.050	1.22
3	1.84	8.45	0.051	1.41
4	1.96	8.34	0.054	1.39

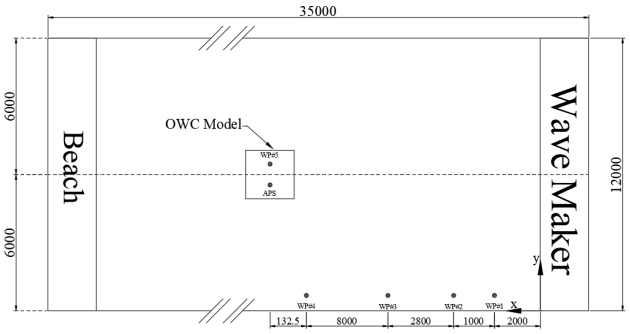

Figure 4. Plan view of experimental layout. Dimensions are in mm [not to scale].

Experimental Data Analysis

The reliability of experimental data was assessed through repeatability tests. As an example, three repeatability tests were conducted for a large steep regular wave with H = 100 mm and T = 1 s ($H \approx 2$ x maximum significant wave height whilst $T \approx T_{owc}$). The time series data recorded by wave probes and air pressure sensor was analyzed and their repeatability was assessed qualitatively and quantitatively with a maximum coefficient of variation value was found to be less than 5%. The 4th order Butterworth low pass filter was used to denoise the signal of wave elevation measured inside the OWC chamber (WP 5) to produce a smooth $V(t)$ signal required to estimate the mean absorbed pneumatic power (P_{out}) using equation (2). The effect of cutoff frequency of 10 Hz and 5 Hz of the filter on the main features of wave data was tested, and the choice of 5 Hz deemed acceptable.

RESULTS

Figure 5 shows the time history of a regular wave test (H = 48.3 mm, and T = 0.93 s). This condition has achieved the highest efficiency of approximately 46.1%. For irregular wave tests, Figure 6 shows a short time history (35 s – 50 s) associated with sea state 1 (H_s = 38 mm, and T_p = 1.335 s) at h_{owc} = 175 mm.

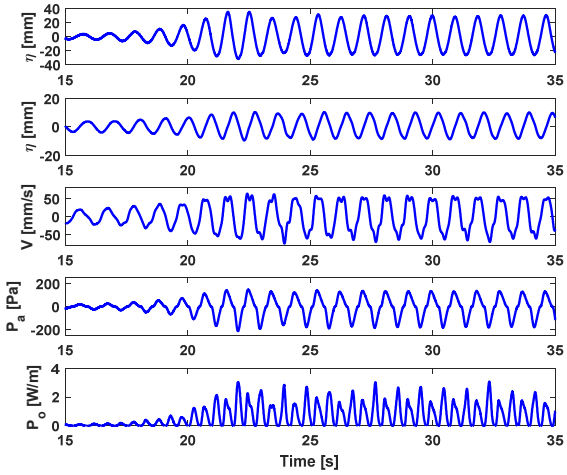

Figure 5. Time history for a regular wave test (H = 48.3 mm, and T = 0.93 s) at h_{owc} = 100 mm. From top to bottom: wave elevation at WP 4; WP 5; OWC velocity; OWC air pressure; and output power.

Compiling all data obtained from regular wave tests at the designed h_{owc} of 100 mm, the WEC's efficiency as per equation (1) was estimated and plotted against the normalized period (T/T_{owc}), as shown in Figure 7.

To study the effect of h_{owc} on the WEC's efficienty, sea state 1 was tested at different h_{owc} values (refer to Figure 2) and the obtained results are summarized in Table 2. The relative change in the OWC WEC's efficincey for cases 2-5 due to reducing h_{owc} from 175 mm (case 1) to 75 mm (case 5) is illustrated in Figure 8.

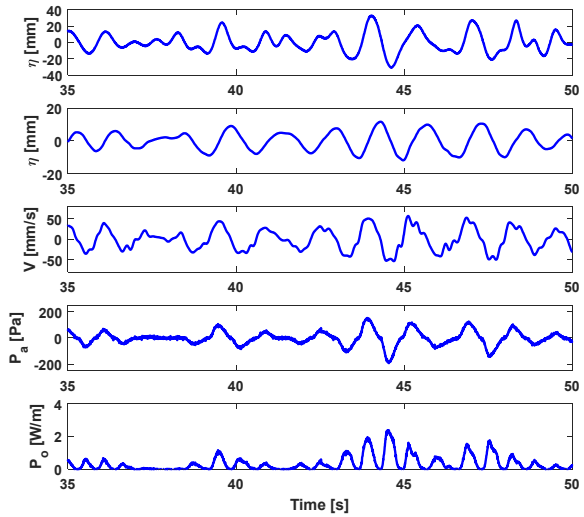

Figure 6. Time history of for sea state 1 (H_s = 38 mm, and T_p = 1.335 s) at h_{owc} = 175 mm. From top to bottom: wave elevation at WP 4; WP 5; OWC velocity; OWC air pressure; and output power.

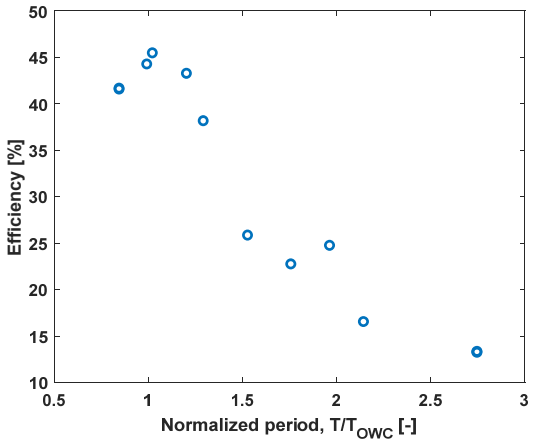

Figure 7. OWC WEC efficiency versus normalized period at h_{owc} = 100 mm.

Table 2. *Obtained efficiencies at different h_{owc} values for sea state 1.*

Case	H_s (mm)	T_p (s)	h_{owc} (mm)	h_{owc}/H_s (-)	T_{owc} (s)	ξ (%)
1	38	1.335	175	4.61	1.063	11.9
2	38	1.335	150	3.95	1.015	13
3	38	1.335	125	3.29	0.964	15.9
4	38	1.335	100	2.63	0.910	16.8
5	38	1.335	75	1.97	0.853	18.8

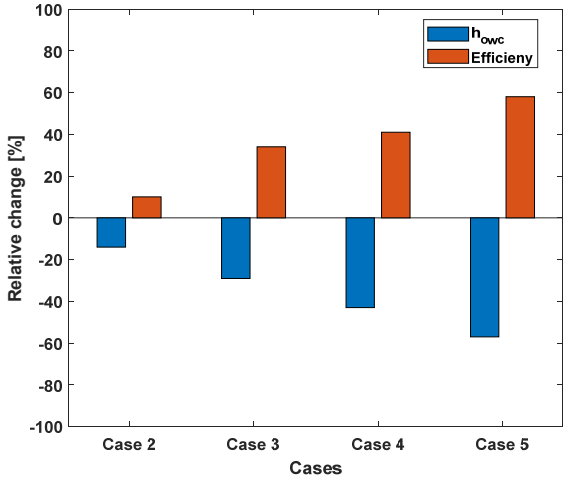

Figure 8. The effect of h_{owc} on OWC WEC's efficiency for sea state 1 (H_s = 38 mm, and T_p = 1.335 s).

DISCUSSION

The representative time history data for regular and irregular wave tests (Figures 5 and 6) provide insights into the OWC's performance under varying wave conditions. One can notice the difference in the power output time history between regular and irregular cases with later being more realistic in terms of power variation over time. For regular wave cases, approximately fully-developed waves (steady-state) were used for power averaging and efficiency estimation. The highest efficiency of the OWC at h_{owc} = 100 mm was observed during regular wave tests at a wave period of 0.93 s (Figure 5), achieving approximately 46.1% efficiency. This peak efficiency aligns with the device's natural period range, confirming the importance of resonance in maximizing energy capture (refer to Table 2 for T_{owc} values).

Figure 7 illustrates the relationship between efficiency and the normalized period (T/T_{owc}). The data reveal that the OWC's efficiency peaks when the wave period is close to the natural period of the OWC, as predicted by equation (4). This highlights the critical role of matching wave characteristics to the OWC's natural frequency for optimal performance.

The effect of varying the OWC WEC's draft (h_{owc}) on the efficiency was examined using sea state 1 (H_s = 38 mm, and T_p = 1.335 s) and showed varying efficiencies with different OWC drafts (h_{owc}). Table 2 and Figure 8 demonstrate a clear trend: as h_{owc} decreases, efficiency increases. The efficiency was observed to decrease as the draft increased: 18.8% efficiency at h_{owc} = 75 mm, 16.8% at h_{owc} = 100 mm, 15.9% at h_{owc} = 125 mm, 13% at h_{owc} =150 mm, and 11.9% at h_{owc} = 175 mm. This inverse relationship is attributed to the reduced water mass within the OWC chamber, which enhances pneumatic pressure generation and reduces the energy required for water column movement.

Using equation (4), Figure 9 further emphasizes the correlation between T_{owc} and h_{owc}. The tested cases (case 1 to

case 5) indicate that as h_{owc} decreases, T_{owc} also decreases, reinforcing the observed efficiency trends. This correlation is crucial for designing OWC devices tailored to specific wave environments to maximize efficiency.

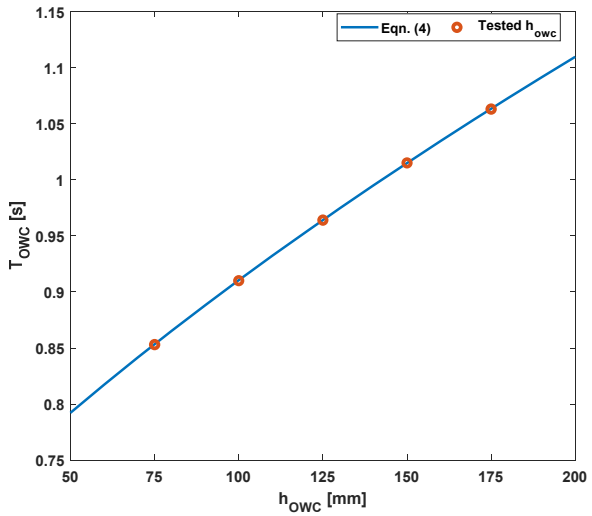

Figure 9. OWC's natural period versus h_{owc}.

Experimental results confirm that energy capture significantly diminishes outside the optimal wave period range. The highest efficiency of approximately 46% was observed for wave periods between 0.8 and 1.2 s, consistent with the natural periods of the device. The calculated peak power output of 0.97 W/m for an input of 2.1 W/m underscores the importance of minimizing these losses to enhance overall efficiency. This finding underscores the need for precise tuning of the OWC's natural period to match the prevalent wave periods at the deployment site. Power losses in the OWC device can be attributed to several factors, including geometric design, air damping, friction, water turbulence, and ambient conditions. Sharp changes in surface direction induce vortex generation, leading to energy losses. Additionally, air damping causes a pressure lag in the OWC chamber, evident at the midpoint of the compression and decompression stages.

In conclusion, the study highlights the critical factors influencing OWC efficiency, including wave parameters, device draft, and the alignment of wave period with the OWC's natural period. These insights are vital for the design and optimization of OWC devices, ensuring efficient and sustainable wave energy conversion.

CONCLUSIONS

This study provides valuable insights into the hydrodynamic performance of a fixed Oscillating Water Column (OWC) Wave Energy Converter (WEC) under various wave conditions, emphasizing the roles of wave period, wave height, and device draft. The experimental results revealed that the peak hydrodynamic efficiency of approximately 46.1% was achieved for a regular wave test with a wave height (H) of 48.3 mm and a wave period (T) of 0.93 s. This peak efficiency occurs at the natural frequency of the water column, confirming the importance of resonance in maximizing energy capture.

The analysis showed a clear correlation between the OWC's natural period (T_{owc}) and its draft, reinforcing the need for precise tuning of the device's natural period to match the prevalent wave periods at the deployment site. The study highlighted that wave steepness significantly affects the device's efficiency, with higher steepness waves generally resulting in lower efficiency due to nonlinear wave behavior.

These findings underscore the critical importance of evaluating site-specific wave conditions for optimal power extraction. By understanding the intricate relationships between wave parameters and OWC performance, this research aids in the geometry optimization and site selection of fixed OWC devices. Overall, the study contributes to the advancement of wave energy conversion technology, promoting the development of efficient and sustainable renewable energy solutions.

ACKNOWLEDGMENTS

The authors are grateful to the University of Doha for Science and Technology (UDST) and the Centre for Maritime Engineering and Hydrodynamics of the Australian Maritime College (AMC), University of Tasmania (UTAS) for facilitating this study. Charlie Rae, Alan Pols, and Dr. Eric Gubesch are also acknowledged.

LITERATURE CITED

DNV. (2010). *Recommended Practice DNV-RP-C205: Environmental conditions and environmental loads*. D. N. Veritas.

Falcão, A. F., & Henriques, J. C. (2016). Oscillating-water-column wave energy converters and air turbines: A review. *Renewable energy*, *85*, 1391-1424.

Molin, B. (2001). On the piston and sloshing modes in moonpools. *Journal of Fluid Mechanics*, *430*, 27-50.

Singh, U., Abdussamie, N., & Hore, J. (2020). Hydrodynamic performance of a floating offshore OWC wave energy converter: An experimental study. *Renewable and Sustainable Energy Reviews*, *117*, 109501.